Large Mammals Have More Powerful Antibacterial Defenses Than Expected from Their Metabolic Rates

Cynthia J. Downs,[1,*] Laura A. Schoenle,[2,†] Eric W. Goolsby,[3] Samantha J. Oakey,[2] Ray Ball,[4] Rays H. Y. Jiang,[2] and Lynn B. Martin[2]

1. Department of Environmental Biology, State University of New York College of Environmental Science and Forestry, Syracuse, New York 13210; 2. Global and Planetary Health, University of South Florida, Tampa, Florida 33620; 3. Department of Biology, University of Central Florida, Orlando, Florida 32816; 4. Department of Biology, Eckerd College, Saint Petersburg, Florida 33711

Submitted February 18, 2022; Accepted July 26, 2022; Electronically published January 4, 2023

Online enhancements: supplemental PDF, video.

ABSTRACT: Terrestrial mammals span seven orders of magnitude in body size, ranging from the <2-g Etruscan pygmy shrew (*Suncus etruscus*) to the >3,900-kg African elephant (*Loxodonta africana*). Although body size profoundly affects the behavior, physiology, ecology, and evolution of species, how investment in functional immune defenses changes with body size across species is unknown. Here, we (1) developed a novel 12-point dilution curve approach to describe and compare antibacterial capacity against three bacterial species among >160 terrestrial species of mammals and (2) tested published predictions about the scaling of immune defenses. Our study focused on the safety factor hypothesis, which predicts that broad, early-acting immune defenses should scale hypermetrically with body mass. However, our three statistical approaches demonstrated that antibacterial activity in sera across mammals exhibits isometry; killing capacity did not change with body size across species. Intriguingly, this result indicates that the serum of a large mammal is less hospitable to bacteria than would be predicted by its metabolic rates. In other words, if metabolic rates underlie the rates of physiological reactions as postulated by the metabolic theory of ecology, large species should have disproportionately lower antibacterial capacity than small species, but they do not. These results have direct implications for effectively modeling the evolution of immune defenses and identifying potential reservoir hosts of pathogens.

Keywords: allometry, antibacterial capacity, constitutive immunity, immune defenses, safety factor hypothesis, scaling.

* Corresponding author; email: cjdowns@esf.edu.

† Present address: Office of Undergraduate Biology, Cornell University, Ithaca, New York 14853.

ORCIDs: Downs, https://orcid.org/0000-0001-9435-0623; Schoenle, https://orcid.org/0000-0002-9591-1194; Goolsby, https://orcid.org/0000-0002-7213-7255; Jiang, https://orcid.org/0000-0001-8982-4169; Martin, https://orcid.org/0000-0002-5887-4937.

Introduction

Hosts can be thought of as islands whose size impacts how many parasites and microbes can colonize them (Kuris et al. 1980). Bigger host species represent bigger islands, leading parasite abundance (Kieft and Simmons 2015), biomass (Poulin and George-Nascimento 2007), diversity (Ezenwa 2004), size (Harrison 1915), size diversity (Poulin 2007), and prevalence (Ishtiaq et al. 2017) to increase with the body size of host species. Large-bodied species also appear more susceptible to some parasite infections (Filion et al. 2020). Furthermore, large body size is intimately connected to the relative value of self-defense versus reproduction (Calder 1984), as most hosts reach large size via a long life span (Harrison 2017; Downs et al. 2020). Altogether, natural selection should favor the evolution of robust immune systems in large hosts (Sheldon and Verhulst 1996; Downs et al. 2014), yet despite a few theoretical (Langman and Cohn 1987; Wiegel and Perelson 2004; Banerjee et al. 2017) and empirical (Lee 2006; Schoenle et al. 2018; Downs et al. 2019) calls to investigate scaling of immune defenses, very little work has yet considered whether and how immune defenses scale across the full range of terrestrial mammalian body sizes.

Body size has been a fruitful theoretical framework for understanding animal design (Prothero 2015). Generally, body size scaling relationships are modeled as power laws, $Y = aM^b$, with linear transformations, $\log_{10} Y = \log_{10} a + b \log_{10} M$, where Y is the focal trait, M is body mass, a is the intercept, and b is the scaling factor. Four hypotheses make predictions about the values of the scaling factors describing the relationship between immune defenses and body mass: (1) protecton, (2) complexity of immunity, (3) rate of metabolism, and (4) safety factor. Each was developed

with a type of immune defense in mind, and different components of the multifaceted and complex immune system likely exhibit different scaling patterns because of different underlying mechanisms and cost-benefit structures (Lee 2006; Downs et al. 2020). These hypotheses are likely not mutually exclusive. Still, as these hypotheses are largely untested and have been broadly applied to immune defenses in the literature (Banerjee et al. 2017; Banerjee 2018; Downs et al. 2020; Ruhs et al. 2020), we test predictions of each herein.

The protecton and complexity of immunity hypotheses both predict that adaptive immune defenses should scale in direct proportion to body size (i.e., isometrically), resulting in an isometric relationship ($b = 0$) for concentration-based immune defenses (e.g., T and B cell concentrations; Langman and Cohn 1987; Wiegel and Perelson 2004). The fractal nature of the circulatory and lymphatic systems is argued to predict isometry of defenses, generally, because rates of parasite detection and delivery of defenses internally should be driven by transit of cells and proteins through the vasculature (e.g., Wiegel and Perelson 2004; Banerjee et al. 2017; Banerjee 2018). Although these frameworks were developed for predicting the number of a single clone of B cells necessary to detect an antigen in a host and circulation time of a B cell (Langman and Cohn 1987; Wiegel and Perelson 2004), they have been extended to other types of induced, adaptive immune defenses (Banerjee et al. 2017; Banerjee 2018).

By contrast, the rate of metabolism hypothesis predicts a hypometric scaling factor for immune defenses ($b < 0$) because biological activities are linked to basal metabolic rates (Brown et al. 2004). As mass-specific basal metabolic rates scale at $b = -0.25$ (i.e., the metabolic activity of single cells of an animal decreases as the size of the species increases), any immune defenses derived from cellular processes and involving cell turnover and protein synthesis should scale similarly (Dingli and Pacheco 2006). This hypothesis was applied to and supported by counts of active hematopoietic stem cell pools (Dingli and Pacheco 2006), the developmental precursors to all immune cells (Kondo et al. 2003). By extension, this hypothesis predicts that synthesis rates of immune molecules are constrained by metabolic rate, so the constitutive humoral concentration of immune defenses should also scale with a scaling factor of -0.25.

Finally, the safety factor hypothesis makes predictions about the scaling of rapid, broadly acting immune defenses as a category. It invokes performance-safety relationships from biophysics (Harrison 2017) and physiology (Diamond 2002) and posits that large species should evolve disproportionately more robust (i.e., hypermetric, $b > 0$) damage mitigation mechanisms than small ones (Harrison 2017; Downs et al. 2020). Immunologically, the safety factor hypothesis predicts that large hosts should evolve exceptionally robust constitutive, broadly acting defenses to protect against the greater infection risks they experience (Downs et al. 2020). Variants of the safety factor hypothesis already exist in the literature, including Peto's paradox for cancer (Peto 1977) and the optimal defense theory (Shudo and Iwasa 2001). Only recently, however, has direct empirical evidence been provided for immune defenses, namely, hypermetric scaling for both neutrophil concentrations in mammals ($b = 0.11$; Downs et al. 2020) and heterophil concentrations in birds ($b = 0.19$; Ruhs et al. 2020). Functionally equivalent and classically considered the first line of immunological defense (Soehnlein 2019), these cells engage in direct antimicrobial activities and produce signals that coordinate subsequent immune responses (Kolaczkowska and Kubes 2013; Mayadas et al. 2014; Schat et al. 2014; Rosales 2018).

Despite evidence for immune allometries for cell concentrations, a morphological trait of the immune system, how and whether functional capacities of constitutive immune defenses scale remain unclear. In other words, it is still obscure whether hypermetric scaling of granulocyte concentrations represents greater immune protection in large animals or evidence that large animals must compensate for lower per-granulocyte effectiveness by circulating more cells. As per-gram metabolism scales hypometrically and cell activities are predicted to scale like per-gram metabolism (Kleiber 1975; Schmidt-Nielsen 1984), the average large-animal leukocyte might be ineffective relative to a leukocyte from a small species. Moreover, as selection tends to act on integrated traits (Bennett and Huey 1990), scaling inference based on functional capacities that affect host fitness (e.g., control of bacterial infections) will inherently be more insightful than studies based solely on cell concentrations.

Our goals here were (i) to determine how sera-based antibacterial defenses scaled with body size among terrestrial mammals by estimating the scaling factor (b) and (ii) to test which hypothesis best predicted the scaling factor for this type of immunity. Antibacterial capacity of sera is an important determinant of host health and virulence for certain bacterial pathogens (Taylor 1983), but it is measurable in a standard way without species-specific reagents (French and Neuman-Lee 2012). Briefly, antibacterial capacity measures the capacity of circulating immune molecules (e.g., lysozyme, mannan-binding protein, β-defensins) to engage the complement cascade, primarily through the alternative pathway, and cause bacteriolysis and bacteriostasis (i.e., the inhibition of bacterial growth; Tieleman et al. 2005; French et al. 2010; Demas et al. 2011). As part of the innate immune system, the complement cascade is initiated quickly upon detection of microbes, and higher constitutive activity should equate with faster detection (Dunkelberger and Song 2010; Iwasaki and Medzhitov 2015).

To describe interspecific variation in this immune function in the most confound-free manner possible, we compared

the efficacy of sera dilutions of several independent replicates from adults of mammalian species housed in zoos. To provide generality to any scaling we observed, we quantified the antibacterial capacity of sera of >160 mammalian species against three distinct bacteria: *Escherichia coli*, *Salmonella enterica*, and *Micrococcus luteus*. These bacteria are common pathogens of many vertebrates (Mastroeni et al. 2001), some portion of their natural infection time line occurs in blood (Mittrücker and Kaufmann 2000), and they are controlled effectively by blood-borne immune defenses (Taylor 1983). Importantly, as their last common evolutionary ancestor was ancient, any consistency in allometries should be more attributable to host immunity than parasite evolutionary history.

To enable meaningful comparisons across species—a substantial challenge for immunity studies—we characterized antibacterial capacity in a dilution series instead of a single dilution of sera (as is typically used; Demas et al. 2011; French and Neuman-Lee 2012). The shapes of resultant *ex vivo* antibacterial functions capture salient aspects of defense, and we made predictions about how each aspect should scale under each scaling hypothesis (fig. 1). Meaningful antibacterial parameters were (i) the maximum concentration of bacteria that serum could protect against as a measure of the upper protective capacity against bacteria, (ii) the serum dilution at the point of most rapid change from protected to vulnerable as a measure of the antibacterial capacity at a single dilution, and (iii) the slope at this steepest part of the bacteriostatic function (fig. 1*A*). This last parameter could be a proxy for how rapidly serum defenses could be recruited to a bacterial replication event (Murphy et al. 2007) or capture the pattern by which proteins and other molecules were recruited combinatorially to control bacteria.

We predict that the safety factor hypothesis will best explain scaling of antibacterial capacity because it focuses on broadly protective, early-acting immune defenses, a category including antibacterial capacity. The safety factor hypothesis predicts that large mammals will have disproportionately greater maximal antibacterial capacity, greater antibacterial capacity at a specific dilution, and a more rapid shift from vulnerable to complete protection than small species (fig. 1*B*). By contrast, the rate of metabolism hypothesis predicts the opposite for large mammals relative to small ones (fig. 1*C*), and the protecton and complexity hypotheses predict that large mammals will have the same antibacterial capacity as small species (fig. 1*D*).

Material and Methods

Samples

We used the simulations performed by Dingemanse and Dochtermann (2013, fig. 1 therein) to guide our choice of sample size. We obtained sera from healthy, zoo- and lab-housed animals ranging in body size from 16 g to 3,600 kg, covering the range of body sizes of extant terrestrial mammals (fig. S1; Smith and Lyons 2011). Although samples from zoo-housed animals comprised the vast majority of our sample, we supplemented these with samples from eight species of lab-housed animals to increase representation of the small-bodied species (<2 kg) in our analysis, as these body sizes are rare for mammals in most zoos. Most zoo samples were collected as part of routine wellness checkups, whereas lab samples were collected at the termination of experiments; all animals from which samples were taken were outwardly healthy. Although captivity itself can affect immune variation in animals (Buehler et al. 2008; Abolins et al. 2011; Viney et al. 2015), scaling factors of leucocyte concentrations for wild ($n = 117$) and captive ($n = 386$) birds were indistinguishable, suggesting that captivity does not affect scaling relationships for some immune defenses (Martin et al. 2022). Final sample sizes of mammal species were 199, 186, and 164 for antibacterial capacity against *Escherichia coli*, *Salmonella enterica*, and *Micrococcus luteus*, respectively; we could not test all of the samples against all of the bacterial species because of serum volume constraints and because sample groups were not completely nested. We assayed a mean of ≥4 samples per species for each microbe ($n = 1$–41 replicates per species; fig. S2). We also obtained >15 samples from a subset of species representing the full range of body masses to ensure that a single individual from a large or small species was not biasing a species mean (table S1; fig. S3) and for a supplemental analysis of how intraspecific scaling changed with body size (i.e., intraspecific scaling; see "Supplemental Analyses" in the supplemental PDF).

Samples were collected in 2005–2019 and stored at −80°C to −20°C at the collection location until shipped on dry ice to our research labs, where they were stored at −80°C until assays. All of the assays were performed within 24 h of thawing samples. Use of these samples was approved by the institutional animal care and use committees (IACUCs) of institutions where samples were obtained. Samples were collected as part of routine veterinary exams under the auspices of IACUCs or the like and were shared after approval by the appropriate committee at each zoo.

Antibacterial Capacity

We measured antibacterial capacity against *E. coli* (ATCC 8739), *S. enterica* (ATCC 13311), and *M. luteus* (ATCC 4698) using an adaptation of the microbiocidal assay developed by French and Neuman-Lee (2012). A full description of the methods is in "Supplementary Methods"

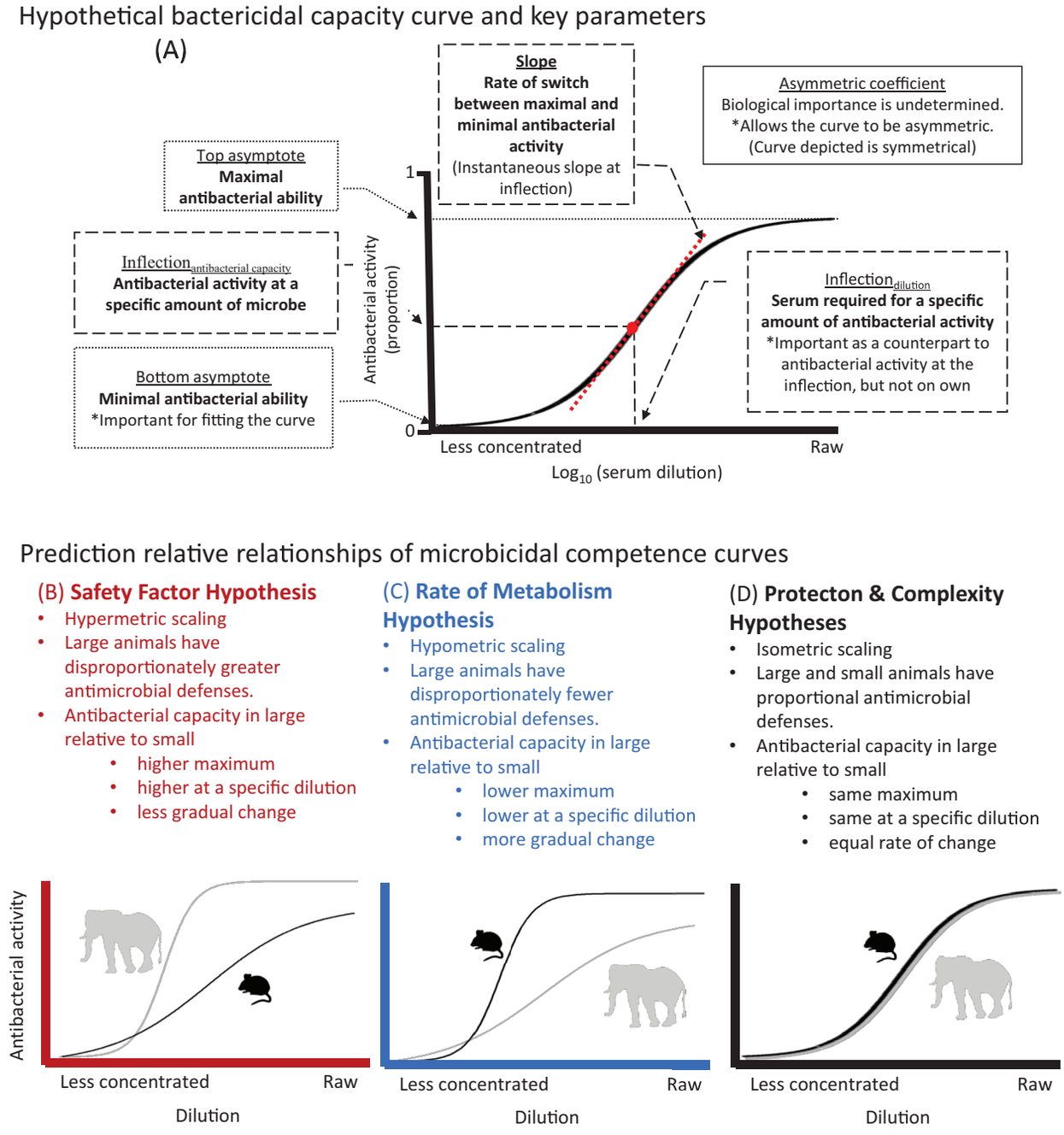

Figure 1: Antibacterial capacity dilution curves. *A*, Hypothetical antibacterial dilution curve showing the parameters we estimated and biological interpretation. This curve shows, names (underlined), and describes the curve parameters and the biological interpretation of the curve parameter (in bold). *B–D*, Hypothetical antibacterial curves for an elephant and mouse showing predictions for the safety factor hypothesis (*B*), the rate of metabolism hypothesis (*C*), and the protecton and complexity hypotheses (*D*).

of the supplemental PDF (summarized in table S2). Briefly, we plated a 12-point dilution curve of each serum sample in triplicate on a round-bottomed 96-well plate. We also plated a four-point dilution curve of commercially available cow serum (Innovative Research, Novi, MI, IBV-Compl) in Dulbecco's phosphate buffered saline (PBS; Sigma-Aldrich D8537) as our interassay control. Our final volume of each serum dilution was 18 μL. We plated three replicates of a 20-μL negative control of PBS and nine replicates of an 18-μL positive control. We added 2 μL of a standard

concentration (10^4 colony-forming units mL^{-1}) of bacteria to all wells except the negative controls. We incubated plates for 30 min at 37°C and then added 125 μL of tryptic soy broth (BD 211825) to all wells and shook plates for 1 min at 300 rpm. We measured baseline absorbance at 300 nm (Biotek Synergy HTX multimode reader) to serve as an internal control before incubating covered plates at 37°C for 10–48 h, depending on the bacteria. We measured final absorbance again at 300 nm and calculated antibacterial capacity for each well as $(1 - (\text{mean}(\text{sample end} - \text{sample baseline})/\text{mean}(\text{positive control start} - \text{positive control end}))) \times 100\%$. Mean interassay and intra-assay variations were 9.0% and 1.9%, respectively, and both were low. Assay protocols are available on Figshare (Schoenle et al. 2020).

Data Processing

All data processing and analyses were performed in the statistical programming language R (R Core Team 2019) using the code developed by Schoenle et al. (2022), Keith et al. (2021), and Downs et al. (2021) and used by Claunch et al. (2022). Code unique to this article is available in the Dryad Digital Repository (https://doi.org/10.5061/dryad.hx3ffbggz; Downs and Martin 2022).

We checked each sample dilution curve for laboratory errors at the levels of the whole plate, replicates within each dilution curve, and the individual dilution curve. First, we subjectively determined whether positive controls, negative controls, and interassay controls (i.e., commercially purchased cow sera) demonstrated the expected patterns (e.g., high optical density [OD] for positive control, the ODs for the most dilute cow sample and positive controls were similar). We discarded a plate and reran samples if the data did not follow the expected pattern. Still, the individuals who performed this step were trained in the criteria and checked regularly (details in Schoenle et al. 2022). Second, we used an R function to identify every instance where a replicate differed from both other replicates independently by >0.1 OD, and if found, we removed that replicate; if all three replicates differed from each other by >0.1 OD, we removed all replicates (Schoenle et al. 2022). Third, we visually examined each dilution curve to check whether it followed the sigmoid shape (Claunch et al. 2022) or a sigmoidal shape with decreased antibacterial activity at a high concentration (*M. luteus* only, indicated by preliminary analysis). If one of the dilutions fell well above or below the rest of the curve, that point was discarded (because we expect dilution curves to demonstrate patterns of more antibacterial capacity to less antibacterial capacity biologically [French and Neuman-Lee 2012; Claunch et al. 2022], and zigzag patterns likely indicated pipetting errors).

We then compiled the data and processed them through a workflow we had developed and previously published (Keith et al. 2021). First, we fitted five-parameter logistic regression curves to each sample's antibacterial capacity curve (i.e., the shape of dilution curves across all 12 serum concentrations) using the package nplr (Commo and Bot 2016; fig. 1*A*). Curves could be fitted only to values between zero and one, so percent inhibited values >100 were forced to a random value between 99 and 100, and values <0 were forced to a random value between zero and one. This approach restricted values to a range near maximal and minimal antibacterial activity observed in other curves. We $\log_{10}$ transformed sera dilutions and converted antibacterial capacity from a percentage to a proportion to aid in curve fitting. We extracted the curve parameters from all curves ($\text{inflection}_{\text{dilution}}$, $\text{inflection}_{\text{antibacterial capacity}}$, bottom asymptote, top asymptote, slope, asymmetric coefficient) to use in univariate and multivariate general linear models (fig. 1*A*). The coefficient of variability (CV) of $\text{inflection}_{\text{dilution}}$ for cow control curves was 4.6% for *E. coli* assays and 10.3% for *S. enterica* assays. The CV for *M. luteus* curves was high but consistently had the expected curve pattern. We suspect this high CV occurred because the middle dilution used in the *M. luteus* curve (dilution = 0.0125) was near the inflection point (estimated mean = 0.021) and curves with steep linear sections are very sensitive to small changes in dilutions; the four-point cow curve was not as sensitive as the 12-point sample curve. Slope and $\text{inflection}_{\text{dilution}}$ were already on a $\log_{10}$ scale. We added 1 to $\text{inflection}_{\text{antibacterial capacity}}$, bottom asymptote, and top asymptote and then $\log_{10}$ transformed them and body mass. All analyses were performed using transformed data.

Data Analyses

Next, we identified scaling factors for the curve parameters and thus for the overall curve shape. Properly estimating scaling factors required models that allowed us to perform multivariate phylogenetic regressions that account for within-species variation. Phylogenetic analyses account for the nonindependence of species (Felsenstein 1985). Importantly for our interest, failing to account for within-species variation can generate inaccurate regression estimates (Garamszegi and Møller 2010; Garamszegi 2014). We employed three different modeling approaches to estimate allometries (summary of each approach in table S3). We interpreted qualitatively consistent results from all models as robust support for those results indifferent to modeling assumptions. For all approaches, we built independent models for antibacterial capacity against each bacterial species. The parameters of biological interest for our hypotheses were $\text{inflection}_{\text{antibacterial capacity}}$, top asymptote, and slope

(fig. 1*A*). We included the bottom asymptote, dilution at the inflection point, and asymmetric coefficient in our statistical models because they inform our understanding of the overall shape of antibacterial capacity curves.

Approach 1: Phylogenetic Covariance. We performed a multivariate phylogenetic comparative analysis for antibacterial capacity against each microbe using the R package Rphylopars (Goolsby et al. 2017, 2021; for code specific to this analysis, see Downs et al. 2021). This approach allowed us to calculate phylogenetic covariances of traits among species while accounting for among-individual variation (Goolsby et al. 2017). Although this approach did not estimate scaling coefficients as they would be estimated with a regression/linear model–based approach, it allowed us to estimate phylogenetic signal of antibacterial capacity and correlations among the antibacterial curve parameters and between curve parameters and body mass within the same model.

All antibacterial capacity curve parameters and body mass were included as response variables in these models, with one exception. Top asymptote was not included in the model for antibacterial capacity against *S. enterica* because it was highly correlated with $\text{inflection}_{\text{antibacterial capacity}}$ ($r = 0.998$, threshold $= 0.9$; but see sensitivity analyses below). We included phylogenetic effects from a tree we produced by pruning the time-rooted tree created by Uyeda et al. (2017) to our species list; we scaled tree height to one. Models were fitted assuming a Brownian motion model of evolution, and we estimated the percentage of variance explained by phylogeny. We tested for phylogenetic signal for each trait using a likelihood ratio test (df $= 1$) by comparing a Pagel's λ model against the null hypothesis of a star phylogeny (i.e., phylogenetic independence of residuals; $\lambda = 0$; Pagel 1997, 1999).

Approach 2: Multivariate Mixed Models. We then built multivariate linear mixed models using the R package MCMCglmm (de Villemereuil and Nakagawa 2014). These models assume that each species is an independent point, and they allowed us to estimate *b* for all curve parameters simultaneously while accounting for within-species variance by including multiple observations per species (Dingemanse and Dochtermann 2013). Being linear models, this approach better paralleled the traditional approach of estimating scaling factors from regression models (Sieg et al. 2009) while utilizing our individual-level data. However, these models did not account for phylogeny because computation run times prohibited their inclusion in such a large data set. (To illustrate, a single phylogenetic multivariate MCMCglmm model for species averages from 150 species [i.e., no within-species variation] took more than 1 month to run on our institution's computer cluster. Adding within-species variation would have increased the running time astronomically.)

We generated separate multivariate mixed models to query body mass effects on antibacterial capacity, one for each bacterial species. All six curve parameters were included as response variables, and we allowed each parameter to have a different slope and intercept. Body mass was included as a fixed effect, and species was incorporated as a random effect. Species had independent intercepts and slopes. These models were fitted using the MCMCglmm package (Hadfield 2010; Hadfield and Nakagawa 2010; de Villemereuil and Nakagawa 2014). All mixed models were fitted using a weak inverse-gamma prior with shape and scale parameters set to 1.002 for the random effect. Default priors for all other fixed effects were used. Model chains were run for 1.82×10^6 iterations, with a 420,000-iteration burn-in and a 1,400-iteration thinning interval. Results were robust across alternative priors, and chain length was sufficient to yield negligible autocorrelation. We extracted the slopes describing the species-level relationship between each parameter and body mass to test our hypothesis about allometries.

Approach 3: Univariate Mixed Models. To test for effects of mammalian phylogeny on antibacterial capacity in a framework based on general linear models, we constructed a separate phylogenetic univariate mixed model for each biologically relevant curve parameter for each bacterium using MCMCglmm (de Villemereuil and Nakagawa 2014). We included body mass and all other curve parameters as fixed effects (Hadfield 2010; Hadfield and Nakagawa 2010). The phylogenetic covariance matrix for this analysis was estimated using a phylogenetic tree constructed with National Center for Biotechnology Information molecular data and phyloT (fig. S4; Letunic 2015). All mixed models were fitted using a weak inverse-gamma prior with shape and scale parameters set to 0.01 for the random effect of phylogenetic variance. Default priors for all other fixed effects were used. Model chains were run for 7.8×10^5 iterations, with a 180,000-iteration burn-in and a 600-iteration thinning interval. We estimated Pagel's λ to measure how much of the total observed variation was explained by phylogeny (Housworth et al. 2004).

Sensitivity Analysis. We conducted additional sensitivity analyses for the multivariate approaches (approaches 1 and 2). Briefly, we reperformed all multivariate analyses after removing variables with a correlation of >0.8 (table S4).

Correlations among Antibacterial Capacity against Different Microbes. We estimated correlations among species means of antibacterial capacity curves against different

bacterial species; we analyzed $\text{inflection}_{\text{antibacterial capacity}}$, top asymptote, and slope in separate modeling exercises. First, we calculated species means for each curve parameter and compared multivariate covariance models with all three curve parameters (e.g., slope of antibacterial capacity against *E coli*, *S. enterica*, and *M. luteus*) using Rphylopars. We used likelihood ratio tests to assess the presence of a phylogenetic signal (as Pagel's λ) in model residuals (Revell 2010). If phylogeny was informative, we performed pairwise, phylogenetically informed covariance models in Rphylopars and used cov2cor to calculate a Pearson correlation. We performed traditional (nonphylogenetic) Pearson correlations in R if phylogeny was not informative.

Results

Overall, mammals exhibit a high diversity of antibacterial curves (video S1), and results from all three modeling approaches were consistent and supported isometric scaling ($b = 0$) for almost all curve parameters of antibacterial capacity against all three microbes. The one exception to this pattern was the slope for antibacterial capacity against *Micrococcus luteus*. In this one instance, all three modeling approaches indicated hypometric scaling such that small animals were disproportionally better able to control this bacterium regarding this one parameter. Results were robust to the removal of the curve parameters with a >0.8 correlation (tables S4–S6).

Phylogenetic Covariance

Models built using Rphylopars estimated that the covariance between body mass and all curve parameters was close to zero and had 95% credible intervals (CIs) that overlapped zero, except one (table 1). The covariance between slope and body mass for antibacterial capacity against *M. luteus* was negative (−11.0; 95% CI: −22.4 to −2.5). The λ values provided evidence of phylogenetic signal in body mass and at least one curve parameter for antibacterial capacity against all three microbes (table 2). Phylogeny explained >92% of variation in body mass but only <10% of the variation in the antibacterial capacity curve parameters of biological relevance (table 2). Phylogenetic and phenotypic covariances can be found in tables S7 and S8, respectively. These models had slightly smaller sample sizes because not all species were in the time-rooted tree. Final sample sizes of species for these models were 191, 178, and 157 for antibacterial capacity against *Escherichia coli*, *Salmonella enterica*, and *M. luteus*, respectively.

Multivariate Mixed Effects Models

Multivariate models generally supported scaling factors of zero for all curve parameters against *E. coli*, *S. enterica*, and *M. luteus*, with two exceptions (table 3; fig. 2). The slope of antibacterial curves against *M. luteus* was hypometric (slope = −4.3; 95% CI: −7.65 to −0.79), and the asymmetric coefficient scaled with a slope of −3.78 (95% CI: −5.60 to −0.91).

Phylogenetic Univariate Mixed Effects Models

Phylogenetic univariate models generally supported scaling factors of zero for all microbes. The 95% CI for all curve parameters for antibacterial capacity against *E. coli*, *S. enterica*, and *M. luteus* overlapped zero except for slope of antibacterial capacity curves against *M. luteus* (table S9), which scaled hypometrically (−4.30; 95% CI: −8.34 to −0.30). Curve parameters were associated with each other (tables S10–S12). Phylogeny explained 1%–18.2% of the variation in antibacterial curve parameters (table S13).

Correlations

Species means of antibacterial capacity against different bacteria were not correlated except for top asymptote of curves

Table 1: Covariance (mean with 95% credible interval) between body mass and antibacterial capacity curve parameters from phylogenetic covariance models estimated using Rphylopars in R

Antibacterial capacity curve parameter	*Escherichia coli*	*Salmonella enterica*	*Micrococcus luteus*
Top asymptote	−.62 (−2.33 to .67)	NA[a]	−.024 (−.11 to .06)
Slope	839 (437 to 1,951)	−.34 (−12.2 to 12.4)	−11.0 (−22.5 to −2.52)
$\text{Inflection}_{\text{antibacterial capacity}}$	−.99 (−2.61 to 0)	.01 (−.17 to .37)	−.02 (−.08 to .37)
$\text{Inflection}_{\text{dilution}}$	−12.2 (−27.0 to −2.26)	−.12 (−.82 to .44)	−.29 (−1.24 to .68)
Asymptote coefficient	1.41 (−2.33 to 5.17)	−.11 (−.33 to .01)	−.03 (−.37 to .17)
Bottom asymptote	−1.05 (−2.64 to −.21)	−.01 (−1.75 to .06)	−.04 (-7.71×10^{84} to 2.13×10^{45})

Note: Top asymptote, $\text{inflection}_{\text{antibacterial capacity}}$, and bottom asymptote were increased by 1 and $\log_{10}$ transformed. Body mass and slope were $\log_{10}$ transformed before β estimation.

[a] Top asymptote was not included in the model for antibacterial capacity against *S. enterica* because it was highly correlated ($r = 0.998$) with $\text{inflection}_{\text{antibacterial capacity}}$. Both variables could not be included in the same model.

Table 2: Values of λ as a test of whether phylogeny was informative and estimates of the percentage of variation in antibacterial curves against *Escherichia coil*, *Salmonella enterica*, and *Micrococcus luteus* explained by phylogeny from phylogenetic covariance models estimated using Rphylopars in R

Antibacterial capacity curve parameter	λ (*P*)			Variance explained (%)		
	E. coli	*S. enterica*	*M. luteus*	*E. coli*	*S. enterica*	*M. luteus*
Body mass	**1 (<.01)**	**1 (<.01)**	**1 (<.01)**	96.6	95.0	92.1
Top asymptote	.01 (1)	NA	.18 (.45)	2.8	NA	6.5
Slope	**.97 (<.01)**	1.00 (.14)	.44 (.02)	9.8	1.4	9.0
$\text{Inflection}_{\text{antibacterial capacity}}$	.08 (.99)	.47 (.36)	.22 (.25)	3.6	6.1	8.1
$\text{Inflection}_{\text{dilution}}$	**1 (<.01)**	**1 (<.01)**	**1 (.02)**	6.9	21.4	4.8
Asymptote coefficient	.75 (.38)	.36 (.49)	.20 (.87)	1.2	1.3	2.1
Bottom asymptote	**.98 (<.001)**	.43 (.162)	.01 (1)	−85.4	4.1	−1.2

Note: Top asymptote, $\text{inflection}_{\text{antibacterial capacity}}$, and bottom asymptote were increased by 1 and $\log_{10}$ transformed. Body mass and slope were $\log_{10}$ transformed before β estimation. Bold text indicates a significant phylogenetic signal.

against *E. coli* and *S. enterica* (table S14). Correlations for $\text{inflection}_{\text{antibacterial capacity}}$ ($\chi^2 < 0.01$, $P = .98$) and top asymptote ($\chi^2 = 0.40$, $P = .53$) were not informed by phylogeny, but slope correlations were ($\chi^2 = 15.9$, $P < .01$).

Strong Support for Isometric Patterns

Isometry of antibacterial capacity was well supported except for the hypometric pattern for slope of antibacterial capacity against *M. luteus* in all analyses. A high slope value indicated that an individual switched from maximal protection against an *M. luteus* infection to almost no protection against it with small changes in bacterial dose around the inflection point of the antibacterial capacity curve. Therefore, hypometric scaling of slope indicated that a large mammal, relative to a small mammal, had a disproportionally slower reduction in defensive capacity with small changes in inoculation dose. In contrast, small and large animals lost protection against *E. coli* and *S. enterica* with the same change in inoculation dose.

Table 3: Estimated intercepts and scaling factors (mode with 95% credible interval) for curve parameters of antibacterial capacity against *Escherichia coil*, *Salmonella enterica*, and *Micrococcus luteus* from multivariate mixed effects models

Antibacterial capacity curve parameter	Intercept		Scaling factor	
	β estimate	Effective sample	β estimate	Effective sample
E. coli:				
$\text{Inflection}_{\text{antibacterial capacity}}$	.18 (.11 to .25)	1,000	.01 (−.01 to .02)	1,124
Slope	42.4 (26.8 to 57.9)	1,000	.98 (−3.26 to 3.89)	1,000
Top asymptote	.27 (.20 to .34)	1,102	.01 (−.01 to .03)	1,000
$\text{Inflection}_{\text{dilution}}$	−.88 (−1.33 to −.52)	1,000	−.03 (−.14 to .04)	1,000
Bottom asymptote	.06 (.01 to .11)	1,000	0 (−.02 to .01)	1,093
Asymmetric coefficient	16.5 (6.7 to 25.1)	1,000	−.68 (−2.54 to 1.50)	1,000
S. enterica:				
$\text{Inflection}_{\text{antibacterial capacity}}$	.22 (.13 to .32)	1,000	0 (−.02 to .02)	1,000
Slope	34.6 (15.4 to 49.8)	901.8	−.38 (−4.42 to 3.48)	898.3
Top asymptote	.31 (.21 to .41)	1,000	.01 (−.02 to .03)	1,000
$\text{Inflection}_{\text{dilution}}$	−.91 (−1.30 to −.56)	886.9	−.03 (−.10 to .06)	887.4
Bottom asymptote	.02 (−.05 to .09)	1,225.3	−.01 (−.02 to .01)	1,220.6
Asymmetric coefficient	24.5 (13.1 to 34.3)	1,000	−3.78 (−5.60 to −.91)	1,000
M. luteus:				
$\text{Inflection}_{\text{antibacterial capacity}}$	.18 (.06 to .33)	1,000	.01 (−.02 to .04)	1,000
Slope	33.2 (14.8 to 46.8)	1,000	−4.31 (−7.65 to −.79)	1,000
Top asymptote	.26 (.10 to .41)	1,000	.02 (−.02 to .05)	1,000
$\text{Inflection}_{\text{dilution}}$	−.73 (−2.03 to .57)	1,000	–.11 (−.40 to .18)	1,000
Bottom asymptote	.07 (−.03 to .28)	1,000	−.03 (−.07 to 0)	1,112
Asymmetric coefficient	4.8 (−13.2 to 17.7)	1,097	1.97 (−1.65 to 4.86)	1,117

Note: Fixed effect is $\log_{10}$ body mass. Top asymptote, $\text{inflection}_{\text{antibacterial capacity}}$, and bottom asymptote were increased by 1 and $\log_{10}$ transformed. Body mass and slope were $\log_{10}$ transformed before β estimation.

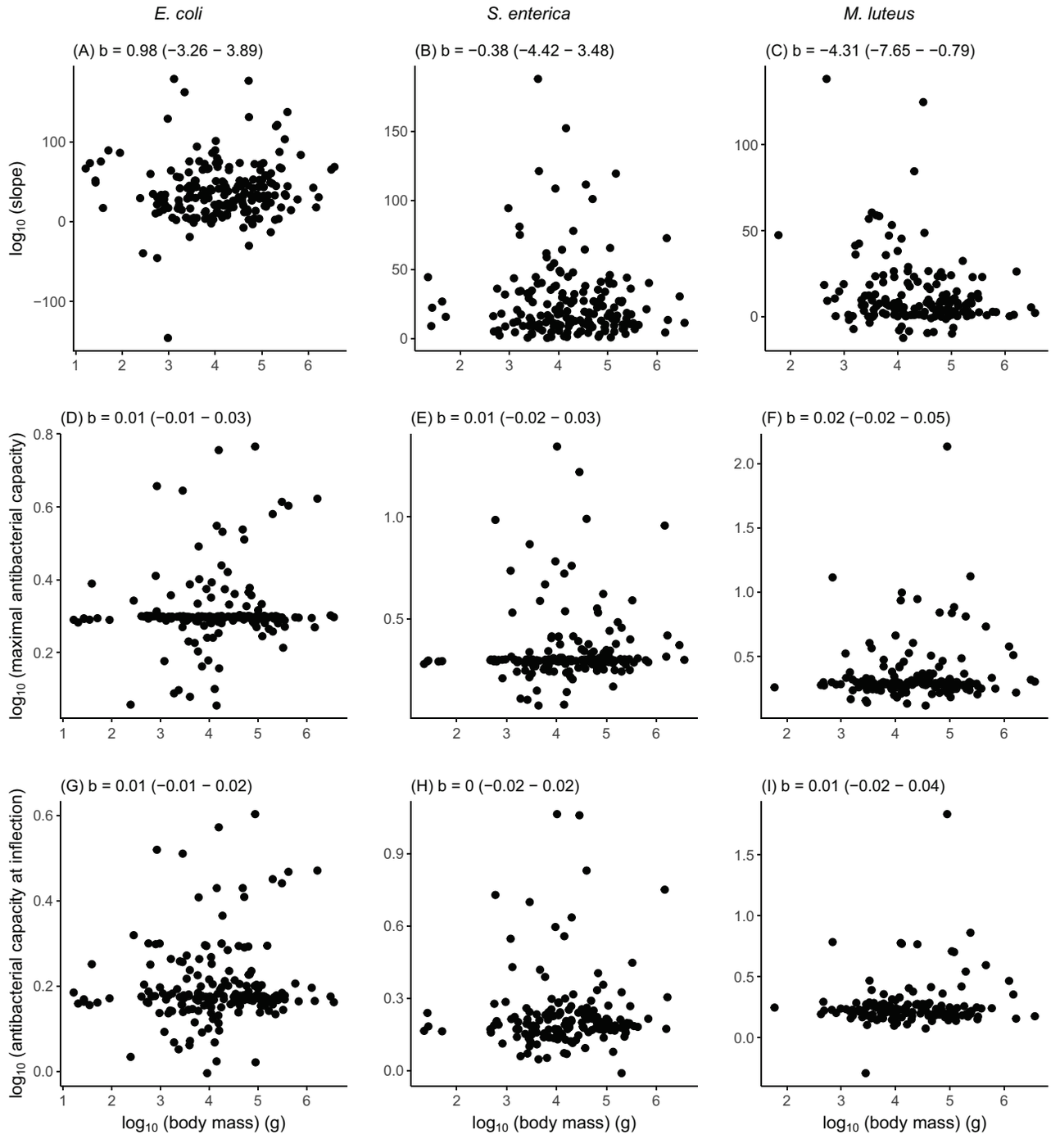

Figure 2: Parameters of antibacterial capacity curves—instantaneous slope at the inflection point (*A*–*C*), maximal antibiotic capacity (*D*–*F*), and antibiotic capacity at the inflection point (*G*–*I*)—against *Escherichia coli* (*A*, *D*, *G*), *Salmonella enterica* (*B*, *E*, *H*), and *Micrococcus luteus* (*C*, *F*, *I*) against body mass. Each point represents a species mean, but analyses were performed on individual-level data.

A prediction of isometric scaling can be challenging to test statistically because it corresponds to a mass-invariant or intercept-only model. A lack of a positive or negative relationship between antibacterial curve parameters and body mass could indicate isometric scaling, or it could indicate that one or both factors are so variable that patterns are hard to discern. We used credible intervals (CIs) or confidence intervals for antibacterial capacity curve parameters with

a priori predictions (e.g., $\text{inflection}_{\text{antibacterial capacity}}$, top asymptote, slope) to distinguish between these alternatives. The ranges of possible true values from the five-parameter curves fitted to the antibacterial capacity curves (i.e., 12-point dilution curves) for $\text{inflection}_{\text{antibacterial capacity}}$ and top asymptote were constrained between zero and one. We defined a narrow 95% CI for these variables as 10% of this range; we considered a 95% CI that overlapped zero and had a range of >0.1 as support for isometric scaling. We expected the range of the 95% CI to be greater for slopes because instantaneous slopes of the five-parameter curves fitted to the antibacterial capacity curves (i.e., 12-point dilution curves) have a wider range of possible values. The theoretical limits of these estimates are $-\infty$ to ∞; we defined narrow ranges as smaller than 10% of 95% of the slope estimates (range of 95% of estimates: 0.14−122; 10% of this range was 12.1).

The 95% CIs of the antibacterial capacity parameters with a priori predictions were narrow, supporting our interpretation that the scaling factors of zero demonstrated true isometry. Specifically, the 95% CI range estimates of the covariance between curve parameters and body mass from the phylogenetic covariance models were <0.02 for $\text{inflection}_{\text{antibacterial capacity}}$ and top asymptote and <0.2 for slope (table 1). Similarly, the 95% CI range for scaling factors derived from multivariate or univariate mixed models was <0.07 for $\text{inflection}_{\text{antibacterial capacity}}$ and top asymptote and <8.04 for slope (tables 3, S10–S12). In contrast, the intraspecific allometries had wide confidence intervals around scaling factor estimates (slope: range ≥ 17.6 wide, mean = 283) and demonstrated no pattern with body size, in general (table S15).

Discussion

Our data provide robust evidence for isometric scaling of serum antibacterial activity among terrestrial mammals and little evidence of a phylogenetic signal. Within each modeling framework, we present nine nonindependent tests of the scaling relationship of antibacterial capacity (3 curve parameters with a priori predictions × 3 microbes). Almost all tests supported the result that antibacterial capacity does not change with body size among species. The one consistent exception was the slope for antibacterial capacity against *Micrococcus luteus*, which was hypometric. We speculate that *Salmonella enterica* and *Escherichia coli* might pose higher risks to mammals than *M. luteus* because *M. luteus* grows slowly and causes modest disease in most hosts relative to the other two bacteria (van der Poll and Opal 2008). Although phylogenetic signal was weak for many aspects of antibacterial capacity, we caution against equating a lack of signal with a lack of evolutionary effects (Blomberg and Garland 2002). Our statistics were designed to test for phylogenetic covariances in extant traits and account for the lack of independence of species-level data (Felsenstein 1985), not for the coevolution of traits.

The species means of antibacterial capacity against different bacterial species were uncorrelated, except for maximal antibacterial capacity against *E. coil* and *S. enterica*. This general pattern of noncorrelation was expected because bacterial species have different population dynamics (van der Poll and Opal 2008) and complement-avoidance strategies (Ramu et al. 2007; Abreu and Barbosa 2017). Additionally, the complement system has three pathways: the classical pathway activated by antibodies, the alternative pathway activated by spontaneous hydrolysis of complement protein 3, and the lectin pathway activated by lectins (Dunkelberger and Song 2010). Different pathways recognize different bacteria, and complement's relative importance in eradicating these bacteria differs (French and Neuman-Lee 2012). For example, *E coli* initiates the classical pathway at lesser concentrations and the alternative pathway at greater concentrations (Li et al. 2008). In contrast, the lectin pathway is activated by *S. enterica* (Gadjeva et al. 2001). We are hesitant to pontificate on the mechanisms underpinning differences in antibacterial capacity against different bacterial species because they have been studied in depth in so few host species.

Generally, isometric scaling supports the protecton and complexity hypotheses. However, these results are somewhat surprising given that large species face a greater risk of infection and greater fitness costs from infections than small species (Downs et al. 2020), and we argue that a higher constitutive antibacterial capacity will lead to faster detection of a bacterial infection. We thus argue below that it is premature to conclude why antibacterial activity of blood scales isometrically. Our results leave open the question of how large mammals can achieve the same functional antibacterial capacity as small mammals, given their disparities in metabolic rates (i.e., mass-specific metabolic rate scaling hypometrically, $b = -0.25$).

Isometric Scaling of Antimicrobial Activity Is Higher Than Expected Given Metabolic Allometries

The isometry of antibacterial capacity is intriguing when considered with the well-documented hypometric scaling of mass-specific metabolic rates (Brown et al. 2004; Savage et al. 2004) and the hypermetric scaling of concentrations of some immune cell types (Downs et al. 2020). The metabolic theory of ecology posits that mass-specific metabolic rate constrains the synthesis of proteins, and indeed, RNA transcriptomes across five species (*Caenorhabditis elegans* to *Danio rerio*) scale hypometrically ($b < 0$). Our assay measured the functional capacity of complement and other

circulating proteins to opsonize and lyse bacteria (Demas et al. 2011; French and Neuman-Lee 2012). Hepatocytes predominantly produce complement proteins in mammals (Zhou et al. 2016; Lubbers et al. 2017), and mammalian hepatocytes scale with a slope of −0.18 (Porter and Brand 1995). As such, complement protein production per hepatocyte should scale at −0.18. Liver mass also scales hypometrically with a slope of 0.895 (Prothero 2015). Because the hepatocyte size is isometric (Savage et al. 2007), large mammals have fewer hepatocytes than small ones. It follows that antibacterial capacity should scale hypometrically. A scaling factor of zero for a concentration-based antibacterial capacity is high within this framework. In other words, large mammals have much higher antibacterial capacity than expected by their metabolic rate alone.

An outstanding question is how large mammalian species obtain the same antibacterial capacity as small ones if they are constrained by metabolism. It could be that as mammals become larger, complement-producing hepatocytes make up a larger portion of their livers, which would result in a trade-off with other liver functions performed by other hepatocytes. Alternatively, complement is a complex system-level response, and the synthesis and release of new complement proteins are regulated by anaphylatoxins produced during a complement response (Haas and van Strijp 2007). The system's dynamics regulating the constitutive concentrations of complement might facilitate the maintenance of the same concentration of complement in large and small mammals regardless of production capacity. Antibacterial capacity is a measure of the constitutive capacity of the complement response (Demas et al. 2011; French and Neuman-Lee 2012). Even if hepatocytes produce complement proteins more slowly in large mammals, the concentration of complement proteins that stops their production might have the same set point across species, resulting in isometric constitutive antibacterial capacity. These potential mechanisms are speculative and are not a comprehensive list.

Isometric Scaling and the Protecton and Complexity Hypotheses

Both the protecton and complexity hypotheses argue that large and small animals need equal defenses against parasites, resulting in some immune responses scaling isometrically (Langman and Cohn 1987; Wiegel and Perelson 2004; Banerjee and Moses 2010), and our results for an innate immune response are generally consistent with this prediction. However, both hypotheses were initially developed to predict how the number of and repertoire of lymphocyte clones should scale with body size to protect against foreign antigens (Langman and Cohn 1987; Wiegel and Perelson 2004; Banerjee and Moses 2010), not to explain constitutive, innate immunity as studied here. We might not expect predictions from these hypotheses to easily transfer to the complement system because it does not have an analogy to B and T cell receptor diversity. Instead, it evolved to be broadly responsive to a wide diversity of foreign substances (Morgan 2000).

Additionally, the adaptive and innate immune systems operate on different timescales (Murphy et al. 2007), and assumptions about the distribution and timing of adaptive immune responses are unlikely to hold for the fast-acting, innate immune defenses, especially constitutive defenses. Lymphocyte responses, the primary cellular components of adaptive responses, require ~4 days to begin responding to a challenge, whereas complement responses are close to immediate (Murphy et al. 2007). The timing of these dynamics suggests different cost and benefit structures for each. It follows that the underpinning logic of the complexity hypothesis would need to be rederived to account for dynamics of innate immune defense and make predictions for broad, early-acting defenses that are part of the innate immune system, such as antibacterial capacity.

Why Isometric Scaling?

Antibacterial capacity and neutrophil concentrations—the other broadly effective constitutive line of mammalian host defense thus far studied in an allometric context ($b = 0.11$; Downs et al. 2020)—have higher scaling factors than expected by scaling of metabolic rates. The safety factor hypothesis posits that these scaling relationships may have evolved because, relative to small mammals, large mammals (1) have a disproportionately higher exposure to parasites and (2) have disproportionately larger discrepancies in biological rates, including defensive ones, relative to rates of invading microbes (Downs et al. 2020). Briefly, large mammals have disproportionately higher exposure risks to parasites because of their ecology and life histories. Relative to small mammals, large mammals consume more food (Nagy 2001; Nunn et al. 2003), have larger home ranges (Lindstedt et al. 1986; Kelt and Van Vuren 2001), are exposed to more habitat with each unit of movement (e.g., step; Schmidt-Nielsen 1984), and have higher absolute exposure to parasites over their lifetimes because they have longer life spans (Peters 1983; Calder 1984; Wiegel and Perelson 2004) than small species. Additionally, parasites have an evolutionary advantage over most hosts because of differences in replication rates and generation times (Downs et al. 2020). Furthermore, selection should favor defenses with short time delays when parasites grow rapidly, as bacterial (and viral) infections often do (Shudo and Iwasa 2001).

Isometric scaling of constitutive antibacterial defenses might be consistent with a broad version of the safety factor

hypothesis. Perhaps instead of predicting hypermetric scaling of all forms of constitutive innate immunity (Downs et al. 2020), the hypothesis should instead focus on the counteracting pressures of parasites and metabolic rate. While selection favors disproportionately greater rapid, broadly acting immune defenses in large animals (Downs et al. 2020), hypermetric scaling of defense may not always evolve because synthesis of immunological molecules and cellular reaction rates might be constrained by metabolic rate (Brown et al. 2004; Savage et al. 2007). Thus, some defenses might scale hypermetrically and some might scale isometrically (or even hypometrically), depending on the system-level regulation, cost-benefit structure, and the mechanistic underpinnings of a defense. This idea is consistent with the observation that large-bodied species appear more susceptible to some parasite infections (Filion et al. 2020) and host disproportionately more parasites (Kieft and Simmons 2015). This broad version of the safety factor hypothesis represents an integration of predictions of the protecton, complexity, rate of metabolism, and narrow safety factor hypotheses.

Conclusion

Our findings suggest that large and small species somehow obtain the same level of protection against bacteria in their blood, at least that mediated by sera. This pattern might also exist in birds; a cross-species comparison of the bactericidal ability—an assay similar to ours but that measures the complement-mediated antibacterial ability of a single dilution of serum or plasma—of 12 bird species also revealed isometric scaling (Tieleman et al. 2005). We are left wondering how large vertebrates maintain the same level of protection as small ones when metabolic rates scale hypometrically. In this manner, a scaling approach revealed an aspect of the design and energetics of the immune system that would not have been revealed otherwise and provides evidence that broad, comparative immunology may help reveal general principles about the architecture of the immune system that traditional ones do not (Martin et al. 2021).

Acknowledgments

We thank Birmingham Zoo, Busch Gardens Tampa Bay (Cara Martel), Cleveland Metroparks Zoo, Columbus Zoo, the Denver Zoological Foundation, Dickerson Park Zoo, Indianapolis Zoo, Lincoln Park Zoo, Louisville Zoological Garden, Maryland Zoo in Baltimore, Milwaukee County Zoo, Naples Zoo, Nashville Zoo at Grassmere, Oregon Zoo (Mitch Finegan, David Shepherdson), Sedgwick County Zoo, Smithsonian's National Zoo and Conservation Biological Institute, Topeka Zoo and Conservation Center, Zoo Atlanta (Hayley Murphy, Stephanie Earhardt), ZooTampa at Lowry Park, and the Demas (Indiana State University), Hoekstra (Harvard University), Ophir (Cornell University), Place (Cornell University), and Monteith (University of Wyoming) labs for donating serum samples. We thank M. Amy, B. Butler, K. Carlson, E. Chinchilli, K. Clausen, H. Droke, M. Espino, A. Fernandez, M. Galan, M. Henning, N. Huizenga, K. Koller, E. Lee, O. Ogunsina, V. Pappademetriou, A. Roberts, C. Stanell, S. Travis, A. Vorrath, R. Winner, C. Yeung for help with laboratory work. N. Keith helped develop the R program workflows required to process our data. We thank N. A. Dochtermann and J. C. Uyeda for statistical guidance and the Martin Lab, H. A. Woods, J. F. Harrison, M. E. Sobolewski, V. Savage, and two anonymous reviewers for discussion about the manuscript. This work was supported by State University of New York College of Environmental Science and Forestry's Provost Office, the Levitt Center, Hamilton College's Dean of Faculty Office, University of South Florida's College of Public Health, and the National Science Foundation (awards IOS-1656551 to C.J.D. and IOS-1656618 to L.B.M.).

Statement of Authorship

C.J.D. and L.B.M. conceptualized the study; L.A.S., S.J.O., C.J.D., and R.B. procured samples; L.A.S., S.J.O., and C.J.D. established and validated the laboratory methodology; L.A.S., S.J.O., C.J.D., and L.B.M. collected and curated the data; C.J.D. carried out the formal analysis with input from L.B.M. and E.W.G.; C.J.D. and L.B.M. drafted the manuscript with input from L.A.S.; all authors contributed to revision; C.J.D. and L.B.M. administered and supervised the project; C.J.D., L.B.M., and R.H.Y.J. acquired funding.

Data and Code Availability

The data sets generated and/or analyzed during the current study were made available to reviewers during review and will be deposited in the Dryad Digital Repository (https://doi.org/10.5061/dryad.hx3ffbggz; Downs and Martin 2022) after a 1-year embargo. We will consider written requests for the data before the end of the embargo. Lab protocols (Schoenle et al. 2020) and general R code (Downs et al. 2021; Keith et al. 2021; Schoenle et al. 2022) referenced herein are available on Figshare. Code specific to this article will be available in the Dryad Digital Repository (https://doi.org/10.5061/dryad.hx3ffbggz; Downs and Martin 2022) after the embargo period.

Literature Cited

Abolins, S. R., M. J. O. Pocock, J. C. R. Hafalla, E. M. Riley, and M. E. Viney. 2011. Measures of immune function of wild mice, *Mus musculus*. Molecular Ecology 20:881–892.

Abreu, A. G., and A. S. Barbosa. 2017. How *Escherichia coli* circumvent complement-mediated killing. Frontiers in Immunology 8:452.

Banerjee, S. 2018. A mathematical framework for understanding how lymph node architecture scales with host body size to produce an efficient immune response. Network Biology 8:90–97.

Banerjee, S., and M. Moses. 2010. Scale invariance of immune system response rates and times: perspectives on immune system architecture and implications for artificial immune systems. arXiv, https://doi.org/10.48550/arXiv.1008.1380.

Banerjee, S., A. S. Perelson, and M. Moses. 2017. Modelling the effects of phylogeny and body size on within-host pathogen replication and immune response. Journal of the Royal Society Interface 14:20170479.

Bennett, A. F., and R. B. Huey. 1990. Studying the evolution of physiological performance. Oxford Surveys in Evolutionary Biology 7:251–284.

Blomberg, S. P., and T. Garland. 2002. Tempo and mode in evolution: phylogenetic inertia, adaptation and comparative methods: phylogenetic inertia. Journal of Evolutionary Biology 15:899–910.

Brown, J. H., J. F. Gillooly, A. P. Allen, V. M. Savage, and G. B. West. 2004. Toward a metabolic theory of ecology. Ecology 85:1771–1789.

Buehler, D. M., T. Piersma, and B. I. Tieleman. 2008. Captive and free-living red knots *Calidris canutus* exhibit differences in non-induced immunity that suggest different immune strategies in different environments. Journal of Avian Biology 39:560–566.

Calder, W. A., III. 1984. Size, function, and life history. Dover, Mineola, NY.

Claunch, N. M., C. J. Downs, L. A. Schoenle, S. J. Oakey, T. Ely, C. Romagosa, and C. W. Briggs. 2022. Snap-freezing in the field: effect of sample holding time on performance of bactericidal assays. Integrative and Comparative Biology, https://doi.org/10.1093/icb/icac007.

Commo, F., and B. M. Bot. 2016. nplr: n-parameter logistic regressions. R package version 0.1-7. https://CRAN.R-project.org/package=nplr.

Demas, G. E., D. A. Zysling, B. R. Beechler, M. P. Muehlenbein, and S. S. French. 2011. Beyond phytohaemagglutinin: assessing vertebrate immune function across ecological contexts. Journal of Animal Ecology 80:710–730.

de Villemereuil, P., and S. Nakagawa. 2014. General quantitative genetic methods for comparative biology. Pages 287–303 *in* L. Z. Garamszegi, ed. Modern phylogenetic comparative methods and their application in evolutionary biology. Springer, Berlin.

Diamond, J. 2002. Quantitative evolutionary design. Journal of Physiology 542:337–345.

Dingemanse, N. J., and N. A. Dochtermann. 2013. Quantifying individual variation in behaviour: mixed-effect modelling approaches. Journal of Animal Ecology 82:39–54.

Dingli, D., and J. M. Pacheco. 2006. Allometric scaling of the active hematopoietic stem cell pool across mammals. PLoS ONE 1:e2.

Downs, C. J., J. S. Adelman, and G. E. Demas. 2014. Mechanisms and methods in ecoimmunology: integrating within-organism and between-organism processes. Integrative and Comparative Biology 54:340–352.

Downs, C. J., N. A. Dochtermann, R. Ball, K. C. Klasing, and L. B. Martin. 2020. The effects of body mass on immune cell concentrations of mammals. American Naturalist 195:107–114.

Downs, C. J., E. W. Goolsby, and L. B. Martin. 2021. Rphylopars code for comparative antimicrobial analysis. Figshare. https://doi.org/10.6084/m9.figshare.14806962.v3.

Downs, C. J., and L. B. Martin. 2022. Data from: Large mammals have more powerful antibacterial defenses than expected from their metabolic rates. American Naturalist, Dryad Digital Repository, https://doi.org/10.5061/dryad.hx3ffbggz.

Downs, C. J., L. A. Schoenle, B. A. Han, J. F. Harrison, and L. B. Martin. 2019. Scaling of host competence. Trends in Parasitology 35:182–192.

Dunkelberger, J. R., and W.-C. Song. 2010. Complement and its role in innate and adaptive immune responses. Cell Research 20:34–50.

Ezenwa, V. O. 2004. Interactions among host diet, nutritional status and gastrointestinal parasite infection in wild bovids. International Journal for Parasitology 34:535–542.

Felsenstein, J. 1985. Phylogenies and the comparative method. American Naturalist 125:1–15.

Filion, A., A. Eriksson, F. Jorge, C. N. Niebuhr, and R. Poulin. 2020. Large-scale disease patterns explained by climatic seasonality and host traits. Oecologia 194:723–733.

French, S. S., D. F. DeNardo, T. J. Greives, C. R. Strand, and G. E. Demas. 2010. Human disturbance alters endocrine and immune responses in the Galápagos marine iguana (*Amblyrhynchus cristatus*). Hormones and Behavior 58:792–799.

French, S. S., and L. A. Neuman-Lee. 2012. Improved *ex vivo* method for microbiocidal activity across vertebrate species. Biology Open 1:482–487.

Gadjeva, M., S. Thiel, and J. C. Jensenius. 2001. The mannan-binding-lectin pathway of the innate immune response. Current Opinion in Immunology 13:74–78.

Garamszegi, L. Z. 2014. Uncertainties due to within-species variation in comparative studies: measurement errors and statistical weights. Pages 157–199 *in* L. Z. Garamszegi, ed. Modern phylogenetic comparative methods and their application in evolutionary biology: concepts and practice. Springer, Berlin.

Garamszegi, L. Z., and A. P. Møller. 2010. Effects of sample size and intraspecific variation in phylogenetic comparative studies: a meta-analytic review. Biological Reviews 85:797–805.

Goolsby, E. W., J. Bruggeman, and C. Ané. 2017. Rphylopars: fast multivariate phylogenetic comparative methods for missing data and within-species variation. Methods in Ecology and Evolution 8:22–27.

———. 2021. Rphylopars: phylogenetic comparative tools for missing data and within-species variation. R package.https://CRAN.R-project.org/package=Rphylopars.

Haas, P.-J., and J. van Strijp. 2007. Their role in bacterial infection and inflammation. Immunologic Research 37:161–175.

Hadfield, J. D. 2010. MCMC methods for multi-response generalized linear mixed models: the MCMCglmm R package. Journal of Statistical Software 33:1–22.

Hadfield, J. D., and S. Nakagawa. 2010. General quantitative genetic methods for comparative biology: phylogenies, taxonomies and multi-trait models for continuous and categorical characters. Journal of Evolutionary Biology 23:494–508.

Harrison, J. F. 2017. Do performance-safety tradeoffs cause hypometric metabolic scaling in animals? Trends in Ecology and Evolution 32:653–664.

Harrison, L. 1915. Mallophaga from *Apteryx*, and their significance; with a note on the genus *Rallicola*. Parasitology 8:88–100.

Housworth, E. A., E. P. Martins, and M. Lynch. 2004. The phylogenetic mixed model. American Naturalist 163:84–96.

Ishtiaq, F., C. G. R. Bowden, and Y. V. Jhala. 2017. Seasonal dynamics in mosquito abundance and temperature do not influence avian

malaria prevalence in the Himalayan foothills. Ecology and Evolution 7:8040–8057.

Iwasaki, A., and R. Medzhitov. 2015. Control of adaptive immunity by the innate immune system. Nature Immunology 16:343–353.

Keith, N. I., L. B. Martin, and C. J. Downs. 2021. Code to compile data and analyze data for a comparative antimicrobial analysis. Figshare. https://doi.org/10.6084/m9.figshare.12430103.v5.

Kelt, D. A., and D. H. Van Vuren. 2001. The ecology and macroecology of mammalian home range area. American Naturalist 157:637–645.

Kieft, T. L., and K. A. Simmons. 2015. Allometry of animal-microbe interactions and global census of animal-associated microbes. Proceedings of the Royal Society B 282:20150702.

Kleiber, M. 1975. The fire of life: an introduction to animal energetics. Rev. ed. R. E. Krieger, Huntington, NY.

Kolaczkowska, E., and P. Kubes. 2013. Neutrophil recruitment and function in health and inflammation. Nature Reviews Immunology 13:159–175.

Kondo, M., A. J. Wagers, M. G. Manz, S. S. Prohaska, D. C. Scherer, G. F. Beilhack, J. A. Shizuru, and I. L. Weissman. 2003. Biology of hematopoietic stem cells and progenitors: implications for clinical application. Annual Review of Immunology 21:759–806.

Kuris, A. M., A. R. Blaustein, and J. J. Alio. 1980. Hosts as islands. American Naturalist 116:570–586.

Langman, R. E., and M. Cohn. 1987. The E-T (elephant-tadpole) paradox necessitates the concept of a unity of B-cell function: the protecton. Molecular Immunology 24:675–697.

Lee, K. A. 2006. Linking immune defenses and life history at the levels of the individual and the species. Integrative and Comparative Biology 46:1000–1015.

Letunic, I. 2015. phyloT: phylogenetic tree generator. https://phylot.biobyte.de/.

Li, K., S. H. Sacks, and N. S. Sheerin. 2008. The classical complement pathway plays a critical role in the opsonisation of uropathogenic *Escherichia coli*. Molecular Immunology 45:954–962.

Lindstedt, S. L., B. J. Miller, and S. W. Buskirk. 1986. Home range, time, and body size in mammals. Ecology 67:413–418.

Lubbers, R., M. F. van Essen, C. van Kooten, and L. A. Trouw. 2017. Production of complement components by cells of the immune system. Clinical and Experimental Immunology 188:183–194.

Martin, L. B., H. E. Hanson, M. E. Hauber, and C. K. Ghalambor. 2021. Genes, environments, and phenotypic plasticity in immunology. Trends in Immunology 42:198–208.

Martin, L. B., E. C. Ruhs, S. Oakey, and C. J. Downs. 2022. Leukocyte allometries in birds are not affected by captivity. Journal of Experimental Zoology A 337:576–582.

Mastroeni, P., J. A. Chabalgoity, S. J. Dunstan, D. J. Maskell, and G. Dougan. 2001. Salmonella: immune responses and vaccines. Veterinary Journal 161:132–164.

Mayadas, T. N., X. Cullere, and C. A. Lowell. 2014. The multifaceted functions of neutrophils. Annual Review of Pathology 9:181–218.

Mittrücker, H.-W., and S. H. E. Kaufmann. 2000. Immune response to infection with *Salmonella typhimurium* in mice. Journal of Leukocyte Biology 67:457–463.

Morgan, B. P. 2000. The complement system: an overview. Pages 1–13 *in* B. P. Morgan, ed. Complement methods and protocols. Vol. 150. Humana, Totowa, NJ.

Murphy, K. P., P. Travers, and M. Walport. 2007. Janeway's immunobiology. 7th ed. Garland Science, New York.

Nagy, K. A. 2001. Food requirements of wild animals: predictive equations for free-living mammals, reptiles, and birds. Nutrition Abstracts and Reviews B 71:R21–R31.

Nunn, C. L., J. L. Gittleman, and J. Antonovics. 2003. A comparative study of white blood cell counts and disease risk in carnivores. Proceedings of the Royal Society B 270:347–356.

Pagel, M. 1997. Inferring evolutionary processes from phylogenies. Zoologica Scripta 26:331–348.

———. 1999. Inferring the historical patterns of biological evolution. Nature 401:877–884.

Peters, R. H. 1983. The ecological implications of body size. Cambridge University Press, New York.

Peto, R. 1977. Epidemiology, multistage models, and short-term mutagenicity tests. Pages 1403–1428 *in* J. D. Watson, H. H. Hiatt, and J. A. Winsten, eds. Origins of human cancer. Cold Spring Harbor Laboratory, New York.

Porter, R. K., and M. D. Brand. 1995. Cellular oxygen consumption depends on body mass. American Journal of Physiology 269:R226–R228.

Poulin, R. 2007. Evolutionary ecology of parasites. Princeton University Press, Princeton, NJ.

Poulin, R., and M. George-Nascimento. 2007. The scaling of total parasite biomass with host body mass. International Journal for Parasitology 37:359–364.

Prothero, J. W. 2015. The design of mammals: a scaling approach. Cambridge University Press, Cambridge.

Ramu, P., R. Tanskanen, M. Holmberg, K. Lähteenmäki, T. K. Korhonen, and S. Meri. 2007. The surface protease PgtE of *Salmonella enterica* affects complement activity by proteolytically cleaving C3b, C4b and C5. FEBS Letters 581:1716–1720.

R Core Team. 2019. R: a language and environment for statistical computing. R Foundation for Statistical Computing, Vienna.

Revell, L. J. 2010. Phylogenetic signal and linear regression on species data: phylogenetic regression. Methods in Ecology and Evolution 1:319–329.

Rosales, C. 2018. Neutrophil: a cell with many roles in inflammation or several cell types? Frontiers in Physiology 9:113.

Ruhs, E. C., L. B. Martin, and C. J. Downs. 2020. The impact of body mass on immune cell concentrations in birds. Proceedings of the Royal Society B 287:20200655.

Savage, V. M., A. P. Allen, J. H. Brown, J. F. Gillooly, A. B. Herman, W. H. Woodruff, and G. B. West. 2007. Scaling of number, size, and metabolic rate of cells with body size in mammals. Proceedings of the National Academy of Sciences of the USA 104:4718–4723.

Savage, V. M., J. F. Gillooly, W. H. Woodruff, G. B. West, A. P. Allen, B. J. Enquist, and J. H. Brown. 2004. The predominance of quarter-power scaling in biology. Functional Ecology 18:257–282.

Schat, K. A., B. Kaspers, and P. Kaiser, eds. 2014. Avian immunology. 2nd ed. Elsevier, Amsterdam.

Schmidt-Nielsen, K. 1984. Scaling: why is animal size so important? Cambridge University Press, Cambridge.

Schoenle, L. A., C. J. Downs, and L. B. Martin. 2018. An introduction to ecoimmunology. Pages 901–932 *in* E. L. Cooper, ed. Advances in comparative immunology. Springer, Cham.

Schoenle, L. A., L. B. Martin, and C. J. Downs. 2020. Protocols for 12-dilution antibacterial capacity curves for interspecific comparisons. Figshare. https://doi.org/10.6084/m9.figshare.12501149.v1

———. 2022. Checking and cleaning data from a 12-point antibacterial curve. Figshare. https://doi.org/10.6084/m9.figshare.18551324.v1

Sheldon, B. C., and S. Verhulst. 1996. Ecological immunology: costly parasite defences and trade-offs in evolutionary ecology. Trends in Ecology and Evolution 11:317–321.

Shudo, E., and Y. Iwasa. 2001. Inducible defense against pathogens and parasites: optimal choice among multiple options. Journal of Theoretical Biology 209:233–247.

Sieg, A. E., M. P. O'Connor, J. N. McNair, B. W. Grant, S. J. Agosta, and A. E. Dunham. 2009. Mammalian metabolic allometry: do intraspecific variation, phylogeny, and regression models matter? American Naturalist 174:720–733.

Smith, F. A., and S. K. Lyons. 2011. How big should a mammal be? a macroecological look at mammalian body size over space and time. Philosophical Transactions of the Royal Society B 366:2364–2378.

Soehnlein, O. 2019. Neutrophil research, quo vadis? Trends in Immunology 40:561–564.

Taylor, P. W. 1983. Bactericidal and bacteriolytic activity of serum against gram-negative bacteria. Microbiological Reviews 47:46–83.

Tieleman, B. I., J. B. Williams, R. E. Ricklefs, and K. C. Klasing. 2005. Constitutive innate immunity is a component of the pace-of-life syndrome in tropical birds. Proceedings of the Royal Society B 272:1715–1720.

Uyeda, J. C., M. W. Pennell, E. T. Miller, R. Maia, and C. R. McClain. 2017. The evolution of energetic scaling across the vertebrate tree of life. American Naturalist 190:185–199.

van der Poll, T., and S. M. Opal. 2008. Host-pathogen interactions in sepsis. Lancet Infectious Diseases 8:32–43.

Viney, M., L. Lazarou, and S. Abolins. 2015. The laboratory mouse and wild immunology. Parasite Immunology 37:267–273.

Wiegel, F. W., and A. S. Perelson. 2004. Some scaling principles for the immune system. Immunology and Cell Biology 82:127–131.

Zhou, Z., M.-J. Xu, and B. Gao. 2016. Hepatocytes: a key cell type for innate immunity. Cellular and Molecular Immunology 13:301–315.

Editor: Daniel I. Bolnick

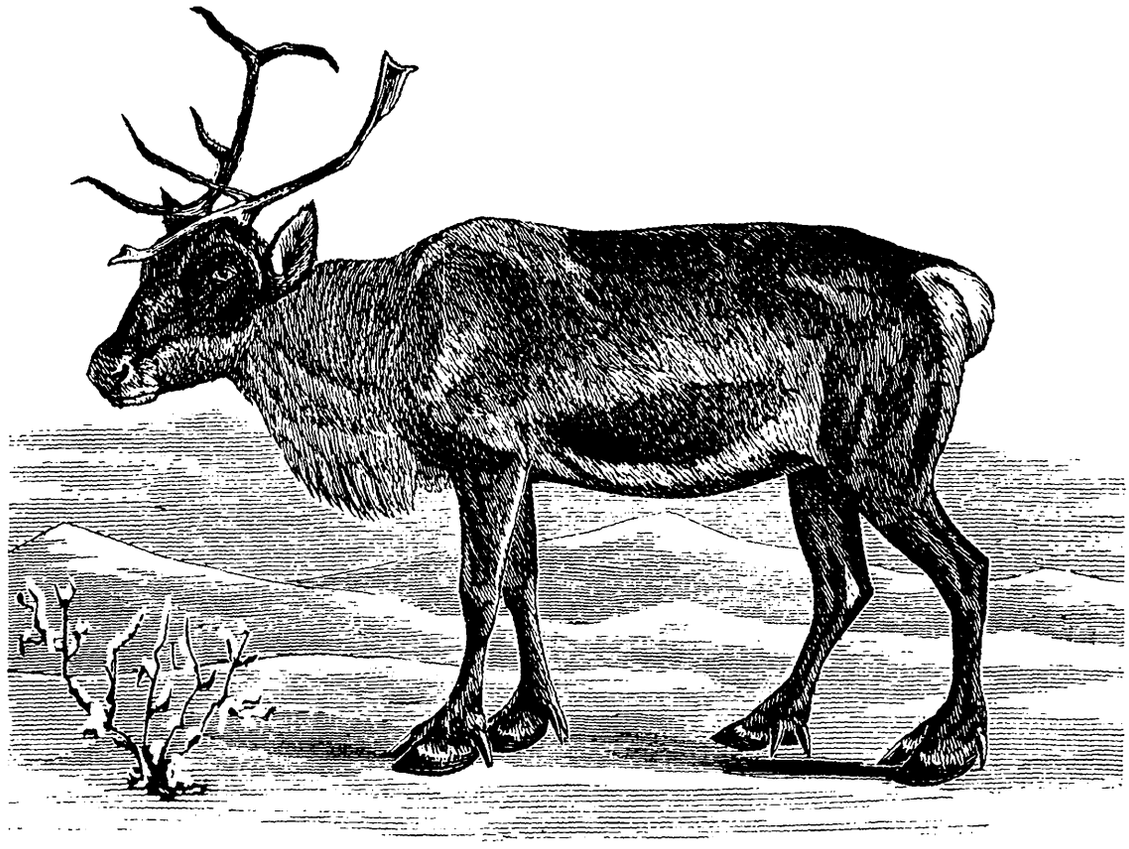

"But of the reindeer and Scandinavian elk our author speaks with the interest and decision of an expert, and his opinion on the specific relations of these animals with our caribou and moose should receive due consideration." Figured: "Wild European reindeer—female." From the review of Caton's *Summer in Norway* (*The American Naturalist*, 1876, 10:39–42).